An observed negative trend in West Antarctic accumulation rates from 1975 to 2010: Evidence from new observed and simulated records

Landon Burgener,[1] Summer Rupper,[1] Lora Koenig,[2] Rick Forster,[3] William F. Christensen,[1] Jessica Williams,[1] Michelle Koutnik,[4] Clément Miège,[3] Eric J. Steig,[5] David Tingey,[1] Durban Keeler,[1] and Laura Riley[1]

Received 31 July 2012; revised 18 March 2013; accepted 21 March 2013; published 28 May 2013.

[1] Observations of snow accumulation rates from five new firn cores show a negative trend that is statistically significant over the past several decades across the central West Antarctic ice sheet (WAIS). A negative temporal trend in accumulation rates is unexpected in light of rising surface temperatures as well as model simulations predicting higher accumulation rates for the region. Both the magnitude of the mean accumulation rates and the range of interannual variability observed in the new records compare favorably to older records collected from a broad area of the WAIS, suggesting that the new data may serve as a regional proxy for recent temporal trends in West Antarctic accumulation rates. The observed negative trend in accumulation is likely the result of a shift in low-pressure systems over the Amundsen Sea region, dominated by changes in the austral fall season. Regional-scale climate models and reanalysis data do not capture the negative trend in accumulation rate observed in these firn cores. Nevertheless the models and reanalyses agree well in both accumulation-rate means and interannual variability, with no single model or dataset standing out as significantly more skilled at capturing the observed magnitude of and trend in accumulation rates in this region of the WAIS.

Citation: Burgener, L., et al. (2013), An observed negative trend in West Antarctic accumulation rates from 1975 to 2010: Evidence from new observed and simulated records, *J. Geophys. Res. Atmos.*, *118*, 4205–4216, doi:10.1002/jgrd.50362.

1. Introduction

[2] The West Antarctic ice sheet (WAIS) is a key contributor to global sea-level rise, with large glaciers along the Amundsen Sea sector, such as Pine Island and Thwaites glaciers discharging the equivalent of 0.2 mm of sea level rise per year [e.g., *Rignot et al*., 2008, *Thomas et al*., 2004; *Wingham et al*., 2009]. The thinning and retreat of the Amundsen Sea sector glaciers are due to both oceanic forcing and changes in glacier geometry [*Joughin et al*., 2010; *Alley et al*., 2005]. Even if discharge rates remain constant, changes to annual accumulation rates over WAIS can also change the ice sheet's mass balance and thus affect global sea level.

[3] Global climate model (GCM) projections of future changes to WAIS accumulation rates suggest that precipitation will increase as temperatures continue to rise [*Genthon et al*., 2009; *Manabe and Stouffer*, 1980; *Thompson and Pollard*, 1997], and an increase in accumulation rates would help mitigate sea level rise [*Oerlemans*, 1982; *Agosta et al*., 2012]. On longer timescales, changes in accumulation rates are likely to play a more complicated role in sea-level change. For example, *Winkelmann et al*. [2012] show that ice flux discharge may increase in response to an increase in snowfall. Thus, quantifying changes in accumulation rates in response to climate variability and climate change is critical to quantifying the contribution of WAIS to future sea-level changes.

[4] Corresponding with GCM projections, recent observations have shown that surface temperatures over WAIS have been increasing by more than 0.1°C per decade since 1957 [*Steig et al*., 2009; *Schneider et al*., 2012], which have been verified independently by borehole temperatures at the central WAIS divide [*Orsi et al*., 2012]. This temperature

Additional supporting information may be found in the online version of this article.

[1]Department of Geological Sciences, Brigham Young University, Provo, Utah, USA.
[2]Cryospheric Sciences Laboratory, NASA Goddard Space Flight Center, Greenbelt, Maryland, USA.
[3]University of Utah, Department of Geography, Salt Lake City, Utah, USA.
[4]Center for Ice and Climate, Niels Bohr Institute, University of Copenhagen, Copenhagen, Denmark.
[5]Department of Earth and Space Sciences, University of Washington, Seattle, Washington, USA.

Corresponding author: S. Rupper, Department of Geological Sciences, Brigham Young University, S389 ESC, Provo, UT 84602, USA. (srupper@byu.edu)

2169-897X/13/10.1002/jgrd.50362

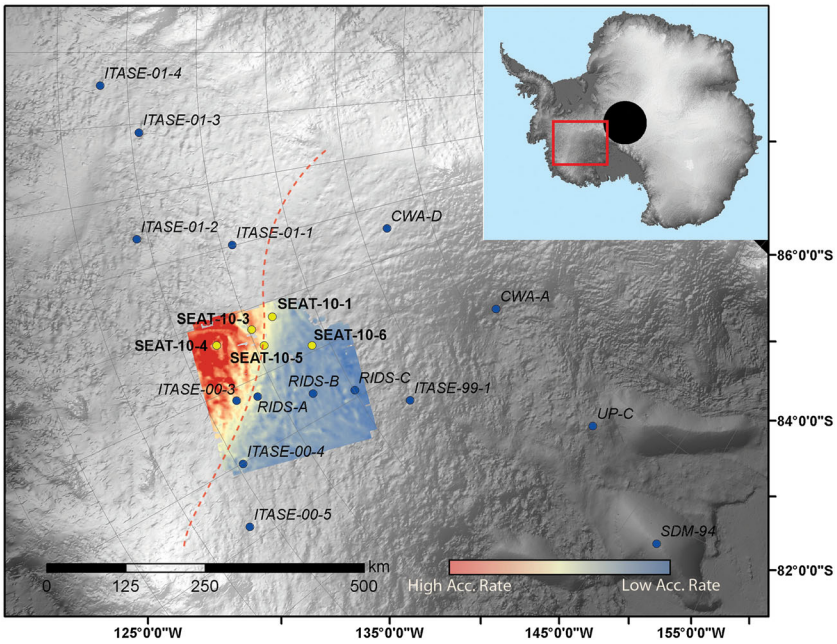

Figure 1. Map showing central WAIS and the SEAT-2010 firn cores (yellow). SEAT-10-1 and ITASE-00-1 are at the same location. Dashed red line marks the approximate position of the WAIS ice divide. Blue points mark cores in the region collected during previous studies. The colored section of the map is modified from *Morse et al.* (2002) and shows the accumulation gradient across WAIS divide from (red) high to (blue) low. Shaded relief map developed from a DEM distributed by the National Snow and Ice Data Center [*Dimarzio et al.*, 2007].

rise might be expected to lead to an increase in precipitation due to the higher saturation vapor pressure of the air masses [*Wallace and Hobbes*, 1977].

[5] Despite the GCM projections and the observed rising temperatures, an increase in accumulation rates across WAIS has not been observed [*Monaghan et al.*, 2006a]. Using isochronous ice layers identified at depth in the ice sheet by airborne radar, *Siegert and Payne* [2004] showed that the 3100-year mean accumulation rates across WAIS divide range between 120 and 200 mm/yr ice equivalent. The suite of 20th century accumulation rates derived from 12 US-ITASE cores in *Kaspari et al.* [2004] give an average of 208 mm water equivalent (w.e.)/yr, suggesting that current accumulation rates are near the long term average. Focusing specifically on trends over the time period of recent warming, *Monaghan et al.* [2006a] showed that WAIS has not experienced any significant trends in accumulation rates since the mid-1950s.

[6] Additionally, a variety of large-, meso-, and small-scale topographic features on the surface of WAIS can contribute to the observed temporal and spatial variability of accumulation and complicate the reconstruction of accumulation rates. In particular, accumulation rates on the leeward side of WAIS divide are lower than accumulation rates on the windward side [*Kaspari et al.*, 2004]. Superimposed on this large-scale pattern is variability due to meso-scale undulations (wavelength > 20 km) [*Kaspari et al.*, 2004]. Cores collected downstream from such undulations may show periods of sustained above- or below-average accumulation rates since deeper portions of the ice/firn cores may have been deposited on the crests or troughs of the undulations. Small-scale wind-formed sastrugi can also affect the uppermost part of firn cores, but these perturbations tend to be eliminated as the layers are buried [*Kaspari et al.*, 2004; *Gow and Rowland*, 1965].

[7] Five new, high-resolution cores were collected in a closely spaced network from a region uncomplicated by meso-scale topographic features. These new cores provide a new accumulation record for the period of WAIS surface warming [*Steig et al.*, 2009] and an opportunity to quantify WAIS accumulation rates over recent decades (~1979 to 2010). The firn cores were collected by the Satellite Era Accumulation Traverse (SEAT) team during the 2010–2011 summer field season (Figure 1).

2. Methods

[8] In 2010, the SEAT team traversed from WAIS Divide Camp towards the Amundsen Sea, crossing the divide, and then returning back to WAIS Divide Camp (Figure 1). Along this route five cores were collected at sites ~70 km apart, ranging across the ice divide (Figure 1 and Table 1). There is a strong accumulation gradient across the divide, with relatively high annual accumulation (>250 mm w.e./yr) on the

Table 1. Geographical Location and Elevation of the Five SEAT-2010 Core Sites

Site	Latitude (N)	Longitude (E)	Elevation (m)
SEAT-10-1	−79.3831	−111.239	1790.7
SEAT-10-3	−79.0416	−111.5456	1772
SEAT-10-4	−78.4879	−111.70007	1649.4
SEAT-10-5	−79.123	−113.042	1793.8
SEAT-10-6	−79.7473	−114.6013	1693.6

coastal side of the divide and low annual accumulation (~150 mm w.e./yr) on the western side [*Morse et al*., 2002; *Vaughan et al*., 1999; *Arthern et al*., 2006]. The five SEAT-2010 core sites were chosen to sample this accumulation gradient over an accessible area.

[9] At each core site, a snow pit was dug through the uppermost layers of snow and firn to a depth where the firn was dense enough to remain intact during drilling (~1.5 m). Density measurements were collected from each of the snow pits with 2 cm vertical resolution. The firn cores were drilled in ~80 cm sections beginning at the base of the snowpits using a FELICS drill [*Ginot et al*., 2002]. Total core depths at the five sites ranged between 15 and 20 m. The sampling process for each core section included obtaining electrical conductivity measurements (ECM), dividing the sections into ~4 cm samples, and measuring the length, diameter, and mass for each sample.

[10] The core sections were shipped to the Glaciology Lab at Brigham Young University. Three to four ECM runs were recorded along each section at a sample-collection rate of 2 cm/s. The sections were then cut into ~2 cm samples, weighed, and measured for density calculations. Cumulative uncertainties for the density calculations are 10% for snowpit samples (as described in *Conger and McClung* [2009]). Cumulative uncertainties for the firn-core samples is approximately 5%, which takes into account the analytical uncertainty of the instruments and the deviation of the core sections from a perfect cylinder. Isotopic analysis ($\delta^{18}O$ and δD) of the melted samples was conducted using a Los Gatos Liquid Water Isotope Analyzer (LWIA-24d) and are normalized to Vienna Standard Mean Ocean Water (VSMOW) and Standard Light Antaractic Precipitation. $\delta^{18}O$ is equal to R/R_{VSMOW} -1, where R is the abundance ratio of $^{18}O/^{16}O$ in water. δD is defined by the same equation, except R is the abundance ratio of D/H in water. Analytical uncertainties for $\delta^{18}O$ and δD are 0.2‰ and 0.6‰, respectively.

[11] Age-depth scales for each core were derived using the seasonal signals of the $\delta^{18}O$ and δD records. ECM and density profiles were used to refine sections of the age-depth scale where the isotopic seasonal cycles were noisy or unclear. In particular, if isotopic peaks were not clearly defined, unusually broad, or contained closely spaced double peaks, the seasonal cycles in density and ECM were combined and used to assess the number and location of likely seasonal peaks. Additionally, the anion concentration of samples contemporaneous with known volcanic eruptions was measured using a Dionex ICS-90 Ion Chromatography System. The resulting solute data were used to quantify the accuracy of the isotope-derived age-depth scale. The two volcanic horizons targeted were the 1991 Pinatubo and 1982 El Chichon eruptions. Four of the cores contained at least one of these prominent peaks; three of the five cores contained both peaks. The Pinatubo peak was dated at 1993 in the SEAT-2010 cores, which corresponds well with observations by *Cole-Dai et al.* [1997] which showed that the majority of Pinatubo sulfate was deposited between 1992 and 1994. The El Chichon sulfate spike occurs in 1983 in the SEAT-2010 cores, approximately 2 years post-eruption. At the two reference horizons, the uncertainty in age for the SEAT-2010 cores is $< \pm 1$ year. Based on the accuracy of the dating around these two reference horizons, the uncertainty in age for the SEAT-2010 cores above the 1991 Pinatubo reference horizons and between the two horizons is estimated to be $< \pm 1$ year; additionally, due to the clean seasonal cycles observed below the 1981 El Chichon sulfate peak, the age uncertainty at depths below the lowest reference horizon is estimated to be ± 1 year. One exception to the above is SEAT-10-4. The seasonal cycle in isotopes and solutes are extremely noisy in this core, and there are no discernible volcanic horizons. The depth-age uncertainty is therefore much greater in this core and difficult to quantify. We include SEAT-10-4 in the figures and analysis of individual cores, but exclude it from the regional averages.

3. Results and Discussion

[12] Figure 2 shows the annual accumulation rates for the five new firn cores collected during the SEAT 2010 field season. The longest record (SEAT-10-6) extends back to 1966 and the shortest record (SEAT-10-5) extends to 1976. The results agree with previous observations [e.g., *Kaspari et al*, 2004], showing a general decrease in accumulation rates with increasing distance from the coast, low correlation between cores over the 1976–2010 period of overlap ($r < 0.36$, p-value > 0.035), and large variation in accumulation rates ($\sigma > 50.9$ mm w.e./yr) in individual cores (Figure S1). Contrasting with the lack of significant accumulation-rate trends reported in other studies [e.g., *Monaghan et al*., 2006a], the results from each of the SEAT-2010 cores show a statistically significant negative trend in accumulation, ranging from a maximum decrease of 72 mm to a minimum of 15 mm w.e. per decade over the past three decades (Figure 2). However, the cores used in these previous studies do not include the most recent 15 years. We will show that the significance of the decrease in accumulation rates in the SEAT-2010 cores is largely influenced by anomalously low accumulation rates in the 1990s and 2000s. Therefore, cores that do not extend into the most recent two decades are unlikely to show a significant trend.

[13] SEAT-10-1 was collected at the International Trans-Antarctic Scientific Expedition core site ITASE-00-1 [*Kaspari et al*., 2004], providing an opportunity to compare the two records, the older of which was collected in 2000. Analysis of the contemporaneous portions of the two accumulation-rate records reveals similar mean accumulation rates (222 and 238 mm/yr w.e., two-tailed *t*-test; $p = 0.33$) and standard deviations (53.3 and 66.5 mm/yr w.e.), but different temporal trends (SEAT-10-1: −2.38 mm/yr w.e., ITASE-00-1: 2.81 mm/yr w.e.). The agreement in mean accumulation rates and interannual variability suggests that the accumulation-rate results for the SEAT-2010 core sites are comparable to previous accumulation-rate observations. However, the difference in trends is large and warrants further discussion. Some of the difference in the accumulation-rate trends may be explained by small spatial-scale variability (<1 km) in snow accumulation. Many studies (e.g., *Genthon et al*., [2005]) have shown that accumulation rates from individual ice cores are greatly affected by these small-scale perturbations; the SEAT-10-1 and ITASE-00-1 cores were likely collected several meters apart due to uncertainties in GPS positioning, which could lead to some differences in accumulation-rate trends. Additionally, uncertainties in the two depth-age scales derived for the different cores could also lead to differences in the reconstructed accumulation-rate records. The large difference in

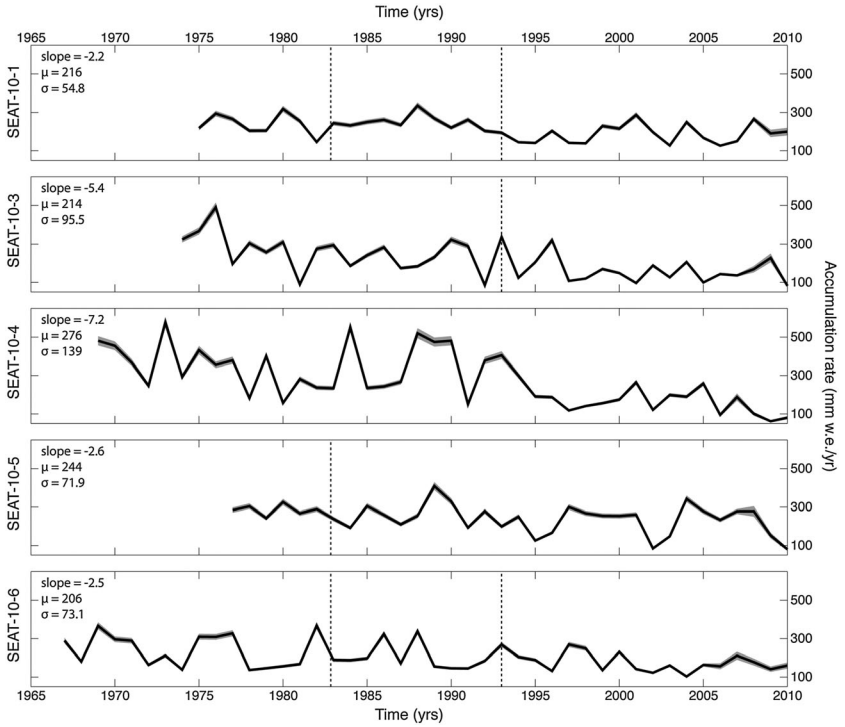

Figure 2. Reconstructed annual accumulation rates (mm w.e./yr). The analytical uncertainty associated with the density measurement for each record is represented by the gray band (10% for snowpit samples, 5% for core samples). Uncertainty associated with the age-depth scale is ±1 year at depth. The dotted lines mark the years 1993 and 1983, correlating with the 1991 Pinatubo 1981 El Chichon volcanic eruptions identified in the cores. Note that all five records show a statistically significant (95% confidence level) negative trend in accumulation rates.

the accumulation-rate trends from these two cores strongly suggests that any trend analysis must (1) make a rigorous accounting of how uncertainties in depth-age scales may affect the results, and (2) the observed trends must occur in multiple cores across the region. The following sections will address both of these factors further.

3.1. Statistical Analysis of Temporal Trends in Accumulation Rate

[14] To evaluate the statistical significance of the trends in accumulation rate, a stacked record was created from the overlapping period of the four cores with greatest confidence in depth-age scales (SEAT-10-1, -3, -5, -6). Note that the inclusion of SEAT-10-4 in the stacked record does not change the statistical significance of the results, but is excluded here as the depth-age uncertainty is much greater than the other cores. *Genthon et al.* [2005] showed that spatially averaging a number of accumulation-rate records together reduces the amount of small-scale noise (noise due to wind redistribution, sublimation) and increases the fraction of common variability between accumulation-rate observations and modeled accumulation rates. Both simple and inverse-variance-weighted averages were created (Figure S2); however, the difference between the results using the two different methods is negligible. The simple average is used in the rest of the study, and referred to hereafter as the stacked record.

[15] To determine whether or not the observed accumulation-rate trends are statistically significant, a regression model accounting for the autocorrelated errors was fit to each of the five normalized accumulation records and to the stacked record. Let the data set of interest be generically referred to as $y = (y_1, y_2, \ldots, y_T)$, where T is the total number of time points. The model for time t is:

$$y_t = \beta_0 + \beta_1 x_t + v_t \tag{1}$$

$$v_t = -\phi_1 v_{t-1} - \phi_2 v_{t-2} - \ldots - \phi_m v_{t-m} + \varepsilon_t \tag{2}$$

$$\varepsilon_t \sim N\left(0, \sigma^2\right) \tag{3}$$

where x_t is the year (time) and v_t is the autocorrelated error term in the regression model. The autoregressive error model parameters ϕ_i govern the nature of the relationship between errors at neighboring times. A first-order autoregressive model for the errors would yield $v_t = -\phi_1 v_{t-1} + \varepsilon_t$, indicating that the error at time t is a function of both the uncorrelated error ε_t and the autoregressive error at the previous time v_{t-1}. When ϕ_1 is a value near -1, then there is a strong positive correlation in the errors from time to time, and the t statistic associated with the test that the null hypothesis ($\beta_1 = 0$) is true will tend to be smaller (less significant) than the standard t statistic associated with the ordinary least squares estimate of the slope. When ϕ_1 is a value near +1, then there is a strong negative correlation in the errors and the t statistic associated with the estimated slope will tend to be larger (more significant) than the standard t statistic associated with ordinary least squares.

Table 2. Statistical Significance of Accumulation Trends (Non-Significant p-Values in *Italics*)

Core/Period	Autoregressive Model	
	t-statistic	p-value
SEAT stack	−7.79	<.0001
Stack from 1980	−4.63	<.0001
Stack from 1990	−2.97	0.0001
SEAT-10-1	−3.80	0.0006
SEAT-10-1 from 1980	−3.61	0.0012
SEAT-10-1 from 1990	−0.23	*0.8216*
SEAT-10-3	−4.52	<.0001
SEAT-10-3 from 1980	−3.71	0.0009
SEAT-10-3 from 1990	−2.15	0.0446
SEAT-10-4	−7.23	<.0001
SEAT-10-4 from 1980	−5.20	<.0001
SEAT-10-4 from 1990	−3.84	0.0011
SEAT-10-5	−3.64	0.001
SEAT-10-5 from 1980	−3.33	0.0026
SEAT-10-5 from 1990	0.38	*0.7098*
SEAT-10-6	−5.20	<.0001
SEAT-10-6 from 1980	−2.08	0.0464
SEAT-10-6 from 1990	−1.10	*0.2852*

[16] For each series y, we fit the ordinary least squares estimate of the slope and recorded the t statistic and p-value. We then ran the autoregressive error model, fitting the model parameters by the maximum likelihood method [*Beach and MacKinnon*, 1978]. The autoregressive error model was chosen by including m lags in the model (equation (2)) (i.e., parameters $\phi_1, \phi_2, \ldots, \phi_{10}$), and then using backward selection to find any autoregressive parameters that have p-values less than 0.10. Table 2 shows the resulting statistics and p-values (95% confidence interval) for each of the records. All of the records show statistically significant negative trends in accumulation rates for the total length of each record (maximum one-sided $p = 0.040$).

[17] Uncertainties in the firn-core depth-age scales introduces errors in the final accumulation rate, which may affect the significance of the trends. Indeed, errors in depth-age scales can lead to partitioning of the snow accumulation of a single year into multiple years (or, conversely, combining multiple years of accumulation into a single year). This can greatly affect both the variability and trends in accumulation

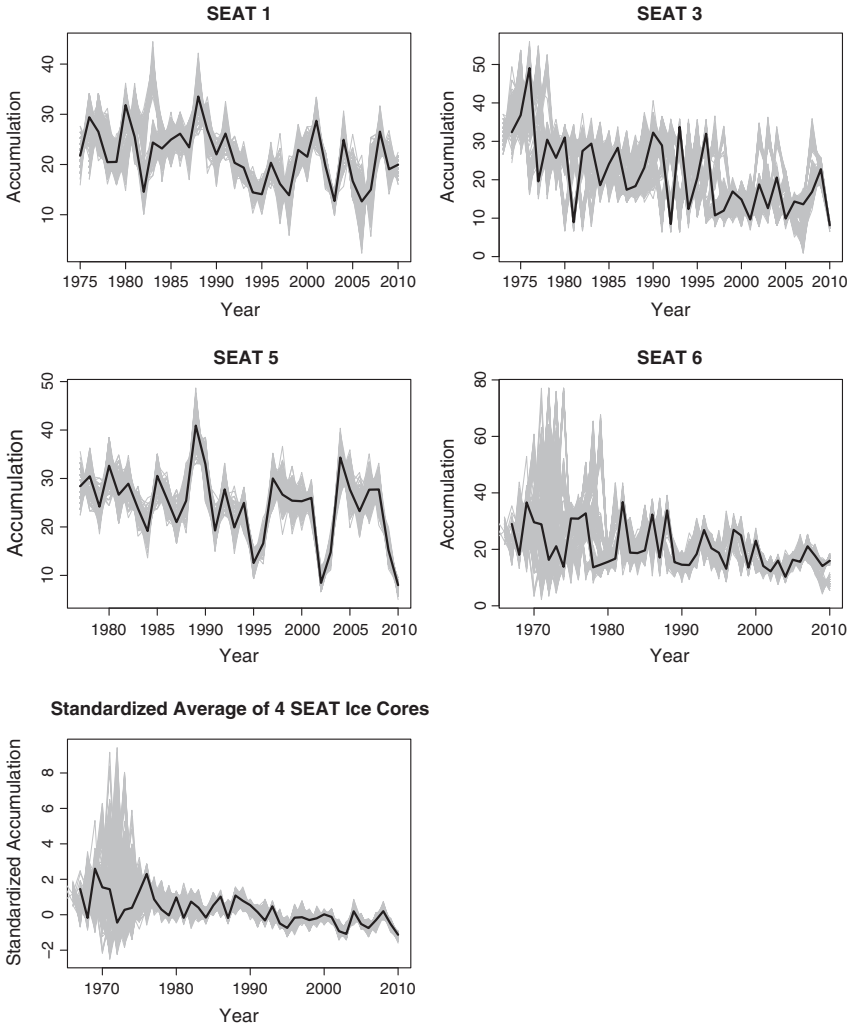

Figure 3. Reconstructed accumulation rates (mm w.e./yr) for each SEAT-2010 core and the stacked record (black) and 1000 possible accumulation rate series based on precision and accuracy uncertainties in the depth-age scale (gray). Note that the negative trend persists in all of the cores at >95% for all of the possible accumulation rate series (see Table 2).

rate when short periods of time are being considered. Therefore, uncertainties in depth-age scales must be considered when testing the significance of trends. Here we generate 1000 different accumulation rates for each core assuming the precision of the date of each isotopic peak is +/− 30–90 days (depending on the morphology of each peak) and the accuracy in the number of years represented in each core is approximately +/- 1 year (Figure 3). Specifically, in the simplest version of the process, the uncertainty in the number of years present in each core is accounted for by first assigning a probability p that each 2 cm firn-core segment is likely to be a midsummer peak. A realization is then drawn from a Bernoulli distribution with probability p to define the possible number of peaks in a given core. Once a given depth-age scale is defined from the Bernoulli trial, a zero-mean normal distribution is assumed for the errors associated with timing of each identified peak within the year. The distribution is assigned based on peak morphology, where well-defined peaks have an assumed standard deviation equal to 30 days, and broad plateaus or noisy peaks have a standard deviation equal to 50 or 90 days depending on the subjectivity of the peak identification. This statistical process is repeated 1000 times for each firn core, resulting in 1000 probable accumulation-rate records for the given depth-age uncertainties for each firn core. Finally, the regression model was applied to the full suite of 1000 accumulation rates for each core and the stacked record to determine the significance of trends in all possible accumulation rate series.

[18] These statistical analyses allowed us to determine if dating errors could explain the negative trends in the accumulation rates. Trends in accumulation rates were statistically significant for >97% of the 1000 accumulation-rate records for all cores and the stacked record (Table 3). Thus, even with the estimated errors in the depth-age scale, the decrease in accumulation rates is statistically significant and reproducible for all cores across the region.

3.2. Deuterium Excess Data

[19] Isotopic data from the firn cores provide additional support for a negative trend in WAIS accumulation rates. Deuterium excess (d-excess) calculated from the isotopic analysis of the SEAT-2010 stacked record shows a statistically significant negative temporal trend (Figure 4). d-excess is often assumed to be a proxy for moisture source region conditions [e.g., *Fernandoy et al*., 2011], though it is also strongly affected by continentality due to the influence of supersaturation under Rayleigh distillation conditions [e.g., *Kavanaugh and Cuffey*, 2003]. In general, it will tend to be more depleted if the distance to the moisture source has decreased, and if the mean moisture source temperature is lower [*Noone and Simmonds*, 2004]. Both of these conditions are met by the reduction in sea ice observed over the last 30 years in the Amundsen-Bellinghausen Seas [*Comiso and Nishio*, 2008; *Parkinson and Cavelieri*, 2012]. The negative d-excess trend is thus consistent with a change in the source region of moisture bearing air masses associated with the overall warming

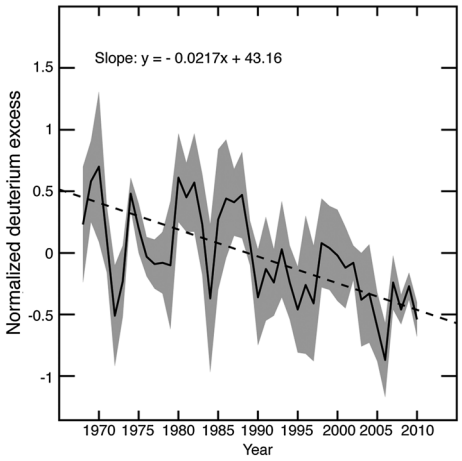

Figure 4. Stacked deuterium excess record from the SEAT-2010 cores. The negative trend in deuterium excess suggests there has been a change in the moisture source region for the study area, consistent with a decrease in sea ice in the Amundsen Sea.

of the WAIS [e.g., *Ding et al*., 2011] that has been accompanied by regional sea ice reductions. While the d-excess data do not provide conclusive evidence of a negative trend in accumulation rates, they do suggest that a change in the moisture source region has occurred, and the sign of that change is consistent with the trend in accumulation-rates in the SEAT-2010 study area.

[20] While uncertainties attend both of these lines of evidence (SEAT-2010 accumulation rates and d-excess), taken together they present a compelling case for decreasing accumulation rates across the SEAT-2010 study area over the past few decades.

3.3. Factors Affecting Accumulation Rate Trends

[21] Possible explanations for the negative trend in accumulation rates, in addition to atmospheric circulation changes, include changes to sublimation/evaporation or wind redistribution of snow, topographic irregularities, and temperature. All of these effects were investigated as possible forcing mechanisms for the observed trends and are explained below.

3.3.1. Topographic Effects

[22] The interpretation of accumulation rates from firn-core records can be influenced by the ice sheet topography upstream of the core site, where undulations on the surface of the ice sheet can be manifested at depth in the core as prolonged periods of above- or below-average accumulation [*Kaspari et al*., 2004]. All five SEAT-2010 cores were collected on or near (distance <75 km) the ice divide, where flow rates are low and surface undulations minimal. Analysis of the topography of the ice sheet upstream from each ice core site was conducted using a 1 km DEM generated from ICESat elevation data [*Dimarzio et al*., 2007] according to the methods described by *Kaspari et al*. [2004].

Table 3. Percent of Possible Accumulation Series With Significant (Two-Sided) Test for Trend

	SEAT-1	SEAT-3	SEAT-4	SEAT-5	SEAT-6	SEAT Stack
Percent Significant	99.90%	100%	100%	97.00%	99.70%	100%

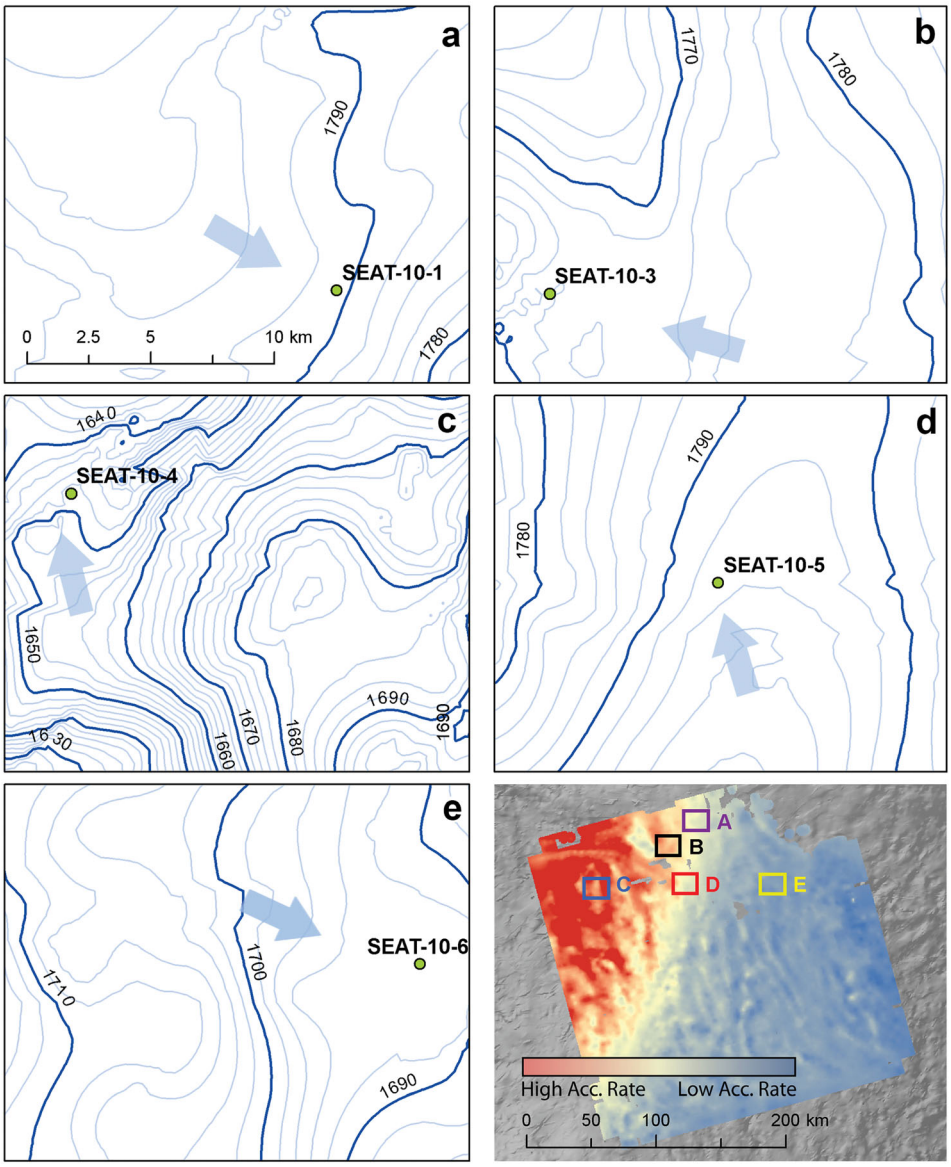

Figure 5. Contour plots showing the topography around the five SEAT-2010 core sites (**a** to **e**). Blue arrows indicate general direction of ice flow. The lower right-hand image shows the accumulation map from *Morse et al.* [2002] as described in Figure 1. SEAT-10-1, SEAT-10-3, SEAT-10-5, and SEAT-10-6 show no signs of upstream undulations that might influence the accumulation rate record. A possible undulation exists upstream of SEAT-10-4, but the core is too short and regional flow rates too slow for the resulting accumulation rate record to be significantly biased. Note that the scale in **a** to **e** are the same.

Figure 5 shows the five SEAT-2010 core sites plotted on a 2 m contour map. Of the five cores, SEAT-10-4 is the furthest from the divide centerline (~73 km) and the only site where the upstream topography is slightly more complex, including a ~10 km wide undulation. The coastward crest of this undulation is 9 km upstream from the core site, and the maximum amplitude between the crest and trough is <6 m. If this undulation has been a stable feature through time, it is possible that the accumulation rates for SEAT-10-4 have been affected by the undulation; however, the ice sheet flow rate near the divide is slow [*Rignot et al.*, 2011; *Conway and Rasmussen*, 2009], and it is unlikely that the 22 m core contains firn old enough to have been significantly affected by the undulation. Additionally, this core is not included in the SEAT-2010 stacked record. When the SEAT-10-4 accumulation-rate record is added to the SEAT-2010 accumulation rate stacked record, the negative accumulation rate trend increases (−3.56 mm w.e./yr vs −2.69 mm w.e./yr when SEAT-10-4).

3.3.2. Temperature Effects

[23] Changes in temperature have a direct effect on saturation vapor pressure (Clausius-Clayperon relationship) and are therefore likely to directly affect accumulation rates. There is no coherent, statistically significant trend in isotope ratios (a temperature proxy) in the SEAT-2010 cores (Figure S3). Certainly, there is no evidence of a negative trend in isotopes (which would imply a negative trend in temperature), which might explain the decrease in accumulation

rates. Additionally, previous studies of the larger WAIS region have shown that temperatures are actually increasing across the larger WAIS area [*Steig et al*., 2009; *Orsi et al*., 2012; *Schneider et al*., 2012; *Küttel et al*., 2012], which would be expected to lead to an increase in accumulation rates. Therefore, the negative trend in accumulation rates cannot be attributed directly to local or regional temperature trends alone.

3.3.3. Wind Redistribution Effects

[24] Changes to wind patterns in the region of the firn cores could lead to wind scouring and sublimation, which could cause a negative accumulation rate trend. While no in situ measurements of wind drift are available for the SEAT-2010 firn cores, model results for the area were investigated. Using the regional climate model RACMO2.1/ANT, *Lenaerts et al*. [2012] show that the region where the SEAT-2010 cores were collected is an area of neutral or depositional snow drifting (~10 mm/yr) for model runs with wind distribution from 1989 to 2009 compared to model runs with no drifting. While this is a slightly shorter time period than the cores, it does not support wind drift patterns causing the negative accumulation rate trends seen in the SEAT-2010 cores. It is noted, however, that little is currently known about wind drift changes on both large and small spatial scales in Antarctica (e.g., *Lenaerts et al*., 2012).

3.4. Relationship Between SEAT-2010 Accumulation Rates and Southern Hemisphere Climate Patterns

[25] Topographic irregularities, temperature change, and wind redistribution of snow do not easily explain the trend in accumulation rates evident in these firn cores. This, in combination with the negative trend in d-excess, supports the hypothesis that changes in direct snow precipitation, forced by changes in atmospheric circulation patterns, over this region are a plausible explanation for the observed negative accumulation-rate trends. The Southern Annular Mode (SAM) is the dominant mode of atmospheric variability in the high latitudes of the Southern Hemisphere and is defined as either the first empirical orthogonal function of sea level pressure, or as the difference in normalized zonally averaged anomalies between 40˚S and 65˚S [*Marshall*., 2003]. Numerous studies have described a positive shift in the SAM since the mid-1970s [e.g., *Thompson et al*., 2011] and linked temporal changes in the SAM to changes in accumulation rates over WAIS [*Genthon et al*., 2003]. However, both *Ding et al*. [2012] and *Schneider et al*. [2012] show that tropical forcing plays a larger role in the climate variability of WAIS than the SAM, although both result in variability in the strength and climatological position of the low-pressure over the Amundsen Sea.

[26] *Genthon et al*. [2003] demonstrated that lower mean sea level pressure (MSLP) over the Amundsen Sea sector would lead to lower precipitation rates over western WAIS (the Ross ice shelf drainage basin) and higher precipitation rates over eastern WAIS (the region of WAIS bordering the Antarctic Peninsula). As shown in Figure 6, this dipole precipitation pattern results from the clockwise rotation of air masses and moisture advection paths around the Amundsen Sea low pressure center, leading to the higher and lower precipitation states in eastern WAIS and western WAIS, respectively. Sustained periods of low accumulation rates across western WAIS observed in the SEAT-2010 accumulation rates records are expected as low-pressure anomalies over the Amundsen Sea occur more often or persist longer. Figure 7 shows the seasonal trends in MSLP from 1979 to 2010 using data from ERA-Interim. Negative trends in MSLP over the Amundsen Sea off the coast of WAIS are occurring throughout the entire year, with the largest negative trend occurring in the fall. However, as this anomaly occurs throughout the entire year, it cannot be simply attributed to the ozone-forced trend in the SAM [*Ding et al*., 2012]. Instead, the anomaly likely reflects a small component of the summer SAM trend, but is dominated by tropical forcing that occurs throughout the rest of the year [*Ding et al*., 2012].

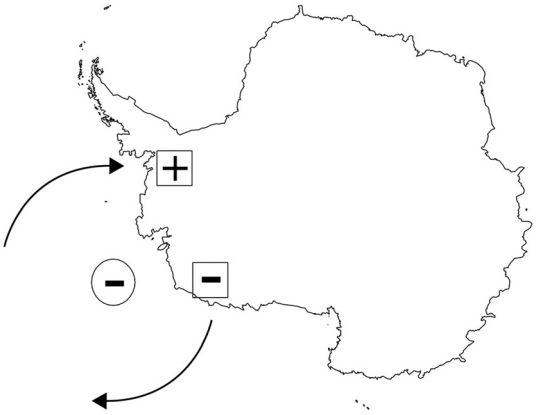

Figure 6. Conceptual image from *Genthon et al*. [2005] showing the effect a low pressure center (minus sign in circle) over the Amundsen Sea has on accumulation rates over WAIS. The low pressure center is associated with the positive phase of the SAM and results in lower accumulation rates over western WAIS (minus sign in square) and higher accumulation rates over eastern WAIS (plus sign in square). As the duration of the low pressure system over the Amundsen Sea has increased, so has the SAM index. This is because the SAM index is strongly determined by the pressure system over the Amundsen Sea.

[27] It is also important to note that although all of the decades covered by the SEAT-2010 ice cores show a negative accumulation rate trend, the magnitude of the negative trend for the complete record is due in large part to the extreme decline in accumulation rates beginning in the 1990s. This shift in accumulation rates is coincident in timing with numerous other observations of shifts in West Antarctic climate. In particular, *Ding et al*. [2011, 2012], *Steig et al*. [2013] and *Fogt and Bromwich* [2006] highlighted shifts in sea surface temperatures, 200 hPa geopotential heights, and atmospheric teleconnections between ENSO and the high latitudes of the Southern Hemisphere during the 1990s. In addition, a phase of acceleration of Pine Island Glacier also occurred in the mid-1990s [e.g., *Joughin et al*., 2003] and is linked to shifts in Circumpolar Deep Water in the Amundsen Sea embayment, particularly in austral fall [e.g., *Wingham et al*., 2009; *Steig et al*., 2012]. Finally, *Steig et al*. [2013] have shown the 1990s isotopic composition of WAIS snow/ice to be anomalous over at least the last 200 years. The coincident shift in accumulation rates is therefore another line of evidence that there was a significant change in climate during the 1990s.

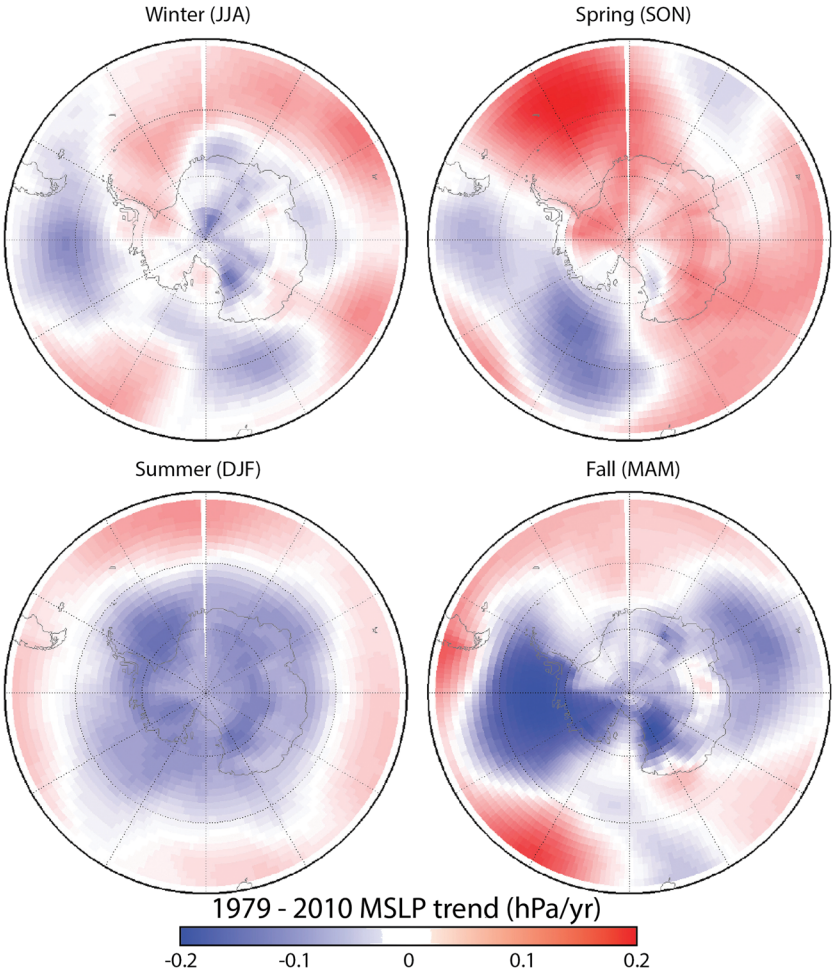

Figure 7. Three-month mean sea level pressure (MSLP) trends in hPa for DJF, MAM, JJA, and SON from 1979 to 2010. Note the negative trends present in the general region of the Amundsen Sea, indicating decreasing MSLP in all seasons. This decrease is dominated by the fall season (MAM). MSLP from ERA-Interim provided by ECMWF.

4. Simulated Versus Observed Accumulation Rates Across Central WAIS

[28] Many different regional climate models and reanalysis datasets (hereafter referred to as simulated records) have been developed to accurately capture Antarctic climate, but it is important to compare these records to observational data in order to determine whether they are capable of capturing the magnitude and variability of accumulation over the ice sheet.

[29] The accumulation rate time series from the SEAT-2010 stacked record was compared to the output generated from two regional climate models (RACMO2.1/ANT [*Lenaerts et al.*, 2012]and Polar MM5 [*Bromwich et al.*, 2004; *Monaghan et al.*, 2006b]), and from three reanalysis datasets (NASA's Modern-Era Retrospective Analysis for Research and Applications (MERRA) [*Reineker et al.*, 2011], ERA-40, and ERA-Interim climate reanalyses generated by ECMWF [*Uppala et al.*, 2005; *Dee et al.*, 2011]). These simulated records calculate accumulation rates differently [*Bromwich et al.*, 2011]. MERRA, ERA-40, ERA-Interim, and the Polar MM5 output used in this study make use of a simple precipitation minus evaporation formula (P – E) that does not take into account various ablation processes such as horizontal transport and sublimation of blowing snow. RACMO2.1/ANT uses a more complex formula to calculate accumulation rates that includes the above-mentioned ablation processes. Figure 8 shows each of these simulated accumulation rates plotted against time. Due to the differences inherent in these simulated records, direct comparison between the individual model grids and the individual/stacked firn cores is beyond the scope of this study. Rather, the regionally averaged accumulation rates in the simulated records are compared to the regionally averaged accumulation rate SEAT-2010 record. The area over which the regional averages were calculated corresponds to the SEAT-2010 study area (77°S to 81°S, 116°W to 120°W).

[30] Figure 8 shows that all of the simulated records are in good agreement with each other over the contemporaneous period (1979-2001). In particular, the simulated records are highly correlated with each other ($r > 0.71$), but are not significantly correlated with the SEAT-2010 stacked record, suggesting that the simulated records are temporally consistent but may not accurately capture the observed variability in accumulation rates (Table 4). However, even if the simulated records were a perfect representation of reality, a high correlation between the simulated records and the stacked

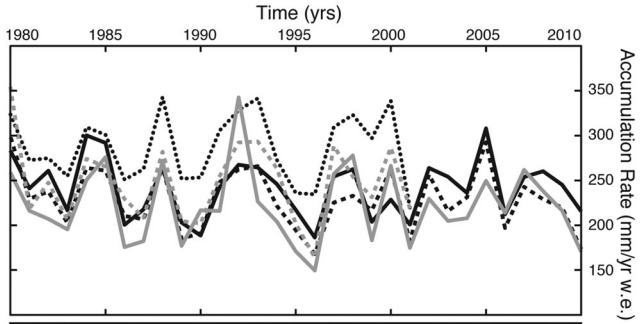

	Merra	ERA-Interim	ERA-40	RACMO2.1/ANT	Polar MM5
Slope	-0.31	-0.64	0.28	-0.07	-0.41
μ	241	228	285	220	245
σ	31.9	33.2	37.7	41.8	43.1

Figure 8. Accumulation rates (mm w.e./yr) simulated for the SEAT-2010 area by three reanalyses and two regional climate models. The magnitude and interannual variability of all of the models/reanalyses are in general agreement. None of the models display a significant trend (positive or negative) in accumulation. It should be noted that all of these models and reanalyses operate on different horizontal grid spacing.

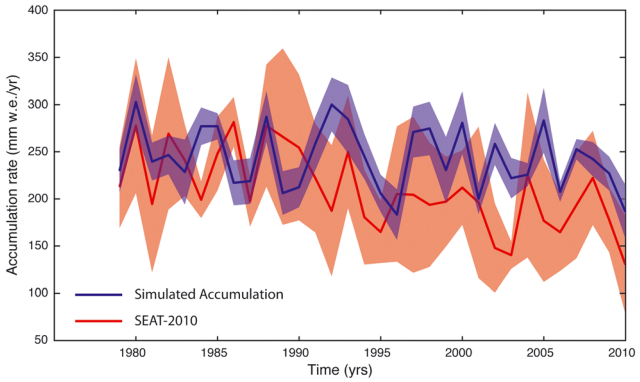

Figure 9. (Red) Observed and (blue) simulated accumulation rates (mm w.e./yr) for the SEAT-2010 study area. Both the observed and simulated time series agree in magnitude and variability, but the simulated record does not capture the large decrease in accumulation rates seen after 1995 in the SEAT-2010 cores. The blue and red bands around each time series mark the 95% confidence intervals.

record may not be expected due to the uncertainties in firn-core accumulation rates (Figure 3). It is perhaps more reasonable to compare the means and the magnitude of interannual variability between the stacked record and the simulated records. With the exception of ERA-40, there is no significant difference in mean accumulation rates between the simulated records and the firn-core stacked record, showing that the simulated records do accurately capture the observed magnitude of accumulation rates. This suggests that despite model differences, no one model/reanalysis is better at simulating mean accumulation rates over the SEAT-2010 study area.

[31] To account for the range of simulated accumulation rates, a multi-model ensemble of the five simulated accumulation-rate records was created for the period 1979 to 2010 by averaging together all models/reanalyses. Figure 8 shows the simulated record ensemble plotted against the stacked SEAT-2010 record, each with their respective 95% confidence intervals. During the 1980s and early 1990s, the ensemble and stacked record agree well in both magnitude and variance; however, the ensemble does not show the sharp accumulation rate decrease apparent in the SEAT-2010 stacked record.

[32] Interestingly, as demonstrated in section 3.4, trends in reanalysis sea level pressure (Figure 7) do show shifts in atmospheric circulation, which would impose a tendency towards decreasing accumulation rates over central and western WAIS. However, as shown above, these large-scale circulation trends do not result in trends in the simulated accumulation rates (Figure 9). Ascertaining in a quantitative way why the simulated records do not reflect the observed trend in accumulation rates is the subject of future work; however, we offer here several possible explanations. First, the simulated records may not be capturing changes in storm frequency and/or intensity associated with the recent changes in synoptic-scale circulation patterns. Or, they may not be capturing the

Table 4. Statistical Comparison of Stacked SEAT-2010 Record and Five Simulated Accumulation Rate Time Series[a]

A	SEAT Stack		MERRA		ERA-INT		ERA-40		RACMO		Polar MM5	
	r	p-value	r	p-value	r	p-value	r	p-value	r	p-value	r	p-value
SEAT Stack	1	0	0.07	0.74	0.25	0.26	0.15	0.50	0.03	0.87	0.22	0.30
MERRA			1	0	0.85	<0.01	0.71	<0.01	0.73	<0.01	0.77	<0.01
ERA-INT					1	0	0.88	<0.01	0.77	<0.01	0.91	<0.01
ERA-40							1	0	0.81	<0.01	0.84	<0.01
RACMO									1	0	0.75	<0.01
Polar MM5											1	0

B	SEAT Stack p-value	MERRA p-value	ERA-INT p-value	ERA-40 p-value	RACMO p-value	Polar MM5 p-value
SEAT Stack	1	0.14	0.62	<0.01	0.86	0.06
MERRA		1	0.30	<0.01	0.15	0.53
ERA-INT			1	<0.01	0.55	0.13
ERA-40				1	<0.01	<0.01
RACMO					1	0.07
Polar MM5						1

[a]Section **A** shows the correlation coefficient (r) and the associated p-value for each record. Section **B** shows the resulting two-tailed p-values from a simple t-test comparing the mean accumulation rate of each record.

magnitude change in large-scale circulation patterns. Another possibility is that increases in sublimation due to circulation changes may not be accurately captured. As mentioned earlier, some of the simulated records do not take into account horizontal snow transport/blowing snow sublimation when calculating accumulation rates, which may lead to differences between the simulated and observed accumulation. However, any trends in these physical processes would also lead to trends in surface sublimation, and no such temporal trends in sublimation are found in the simulated data, suggesting that the inclusion of additional ablation processes in the model/reanalysis schemes would not have a large effect on the simulated accumulation rates. Indeed, RACMO2.1/ANT, which does include these ablation processes in its calculation of accumulation, does not show a higher negative trend in accumulation rates than the other simulated records. If there is a significant change in wind velocity not captured by the models, then all models and reanalysis data may be underestimating changes in sublimation, regardless of the complexity of the sublimation schemes.

5. Conclusions

[33] The negative accumulation-rate trend observed in all of the SEAT-2010 cores may be unexpected in light of increasing temperatures across WAIS [*Steig et al*., 2009; *Orsi et al*, 2012; *Schneider et al*., 2012; *Küttel et al*., 2012]. The combined mean of the five SEAT-2010 cores suggests that on average, accumulation rates have been decreasing across the region, on average, by 3.8 mm w.e./yr, with significant declines in accumulation rates beginning in the mid-1990s. Statistical analysis shows that the negative trend is statistically significant at the 95% confidence interval for all five cores and the stacked record.

[34] d-excess is an additional line of evidence suggesting that the SEAT-2010 study area has experienced changes in precipitation source regions associated with the decrease in accumulation rates over the past four decades. In particular, d-excess reconstructed from the isotopic analysis of the SEAT-2010 cores shows a statistically significant negative trend that may be due to a decrease in sea ice in the Amundsen Sea. The observed sea ice decrease in the Amundsen Sea and sea ice increase in the Ross Sea [*Turner et al*., 2009] are consistent with the change in atmospheric circulation patterns this study cites as a mechanism for decreases in accumulation rate.

[35] No clear trend exists in the $\delta^{18}O$ and δD isotopic records, suggesting that the decrease in accumulation rates cannot be readily explained by a regional trend in temperature. Additionally, it is unlikely that the negative trends are the direct result of topography. SEAT-10-4 is the only site where surface undulations exist, and due to the short time period covered by the core, these undulations are unlikely to have affected the reconstructed accumulation rates. Finally, while the magnitude of the accumulation change presented here could be explained by changes in wind redistribution of snow, current models do not support a change in wind scouring of snow in this region; however, direct measurements are needed to verify this modeled result.

[36] One possible explanation for the decreasing accumulation rates is a change in atmospheric circulation patterns influencing precipitation over central WAIS. A negative trend in sea level pressure has been observed over the Amundsen Sea region since the 1970s (with the largest changes occurring in austral fall). *Genthon et al*. [2003] showed that this low-pressure system over the Amundsen Sea is directly linked to lower moisture advection and thus reduced precipitation over western WAIS. If the negative trend in accumulation rates in the SEAT-2010 cores is indeed the result of the year-round negative trend in sea level pressure, this may suggest that the shift towards lower snow precipitation is the result of changes to tropical Pacific sea surface temperatures that affect atmospheric circulation patterns over the Amundsen Sea region throughout the year [e.g., *Ding et al*., 2012], and changes to atmospheric dynamics at high latitudes (as evidenced by the positive trend in the SAM) during the summer months [e.g., *Marshall*, 2003].

[37] While there are trends in atmospheric circulation that tend to decrease accumulation rates over western and central WAIS, these accumulation-rate trends are not captured in the two regional climate models and three reanalysis datasets used in this study. In particular, the observed and simulated accumulation rates diverge sharply after 1995, suggesting the models/reanalyses do not adequately capture precipitation variations with atmospheric circulation over central WAIS. No single model or reanalysis dataset is more skilled at simulating either mean accumulation rates or accumulation-rate trends over the SEAT-2010 study area, regardless of the spatial resolution or model details.

[38] Though the negative trend in accumulation rates is statistically significant, the cores do not cover a long enough period to determine if this is a long-term shift in climate over central WAIS. It is possible that longer-term temperature increases will eventually result in an increase in snow accumulation, but this slow increase in accumulation rates is not yet observable over the decadal variability. It is equally plausible that due to regional circulation patterns, an increase in temperature will not lead to a uniform accumulation-rate increase over WAIS and may even result in decreases in accumulation over large regions despite increases in temperature. Another possibility is that trends in atmospheric conditions over the Amundsen Sea region and WAIS may be linked to anthropogenic forcing of tropical Pacific sea surface temperatures [*Ding et al*., 2012]. If so, future accumulation rates over central WAIS may continue to decrease as greenhouse gases continue to rise. This suggests that models will have to correctly capture the trends and variability in the tropical Pacific in order to accurately simulate trends and variability in WAIS accumulation.

[39] **Acknowledgments.** This work was supported by the National Science Foundation Office of Polar Programs (grant 094470 to SBR and 0944653 to RF) and NASA's Cryospheric Sciences Program (to LSK). The authors thank David Battisti and Qinghua Ding for feedback on the methods and science. The authors also thank three anonymous reviewers for constructive comments and criticisms that significantly improved the manuscript.

References

Agosta, C., V. Favier, C. Genthon, H. Gallée, G. Krinner, J. T. M. Lenaerts, and van den Broeke, Michiel R. (2012), A 40-year accumulation dataset for Adelie Land, Antarctica and its application for model validation, *Clim. Dyn.*, *38*, 75–86, doi:10.1007/s00382-011-1103-4.

Alley, R. B., P. U. Clark, P. Huybrechts, and I. Joughin (2005), Ice-sheet and sea-level changes, *Science*, *310*, 456–460, doi:10.1126/science.12114613.

Arthern, R. J., D. P. Winebrenner, and D. G. Vaughan (2006), Antarctic snow accumulation mapped using polarization of 4.3-cm wavelength microwave emission, *J. Geophys. Res.*, *111*, D06107, doi:10.1029/2004JD005667.

Beach, C. M., and J. G. MacKinnon (1978), A maximum likelihood procedure for regression with autocorrelated errors, *Econometrica*, *46*, 51–58.

Bromwich, D. H., Z. Guo, L. Bai, and Q. Chen (2004), Modeled Antarctic Precipitation. Part I: Spatial and Temporal Variability, *J. Clim.*, *17*, 427–447, doi:10.1175/1520-0442(2004)017 < 0427:MAPPIS > 2.0.CO;2.

Bromwich, D. H., J. P. Nicolas, and A. J. Monaghan (2011), An assessment of precipitation changes over Antarctica and the Southern Ocean since 1989 in contemporary global reanalyses, *J. Clim.*, *24*, 4189–4209, doi:10.1175/2011JCLI4074.1.

Cole-Dai, J., E. Mosley-Thompson, and L. Thompson G (1997), Quantifying the Pinatubo volcanic signal in south polar snow, *Geophys. Res. Lett.*, *24*, 2679–2682, doi:10.1029/97GL02734.

Comiso, J. C., and F. Nishio (2008), Trends in the sea ice cover using enhanced and compatible AMSR-E, SSM/I, and SMMR data, *J. Geophys. Res.*, *113*, C02S07, doi:10.1029/2007JC004257.

Conger, S. M., and D. M. McClung (2009), Instruments and methods comparison of density cutters for snow profile observations, *J. Glaciol.*, *55*, 163–169, doi:http://dx.doi.org/10.3189/002214309788609038.

Conway, H., and L. A. Rasmussen (2009), Recent thinning and migration of the Western Divide, central West Antarctica, *Geophys. Res. Lett.*, *36*, L12502, doi:10.1029/2009GL038072.

Dee, D. P., et al. (2011), The ERA-Interim reanalysis: configuration and performance of the data assimilation system, *Q. J. Roy. Meteorol. Soc.*, *137*, 553–597, doi:10.1002/qj.828.

Dimarzio, J., A. Brenner, H. Fricker, R. Schutz, C. A. Shuman, and H. J. Zwally (2007), GLAS/ICESat 500 m laser altimetry digital elevation model of Antarctica, *Natl. Snow and Ice Data Cent., Boulder, Colo., 2012*.

Ding, Q., E. J. Steig, D. S. Battisti, and M. Küttel (2011), Winter warming in West Antarctica caused by central tropical Pacific warming, *Nat. Geosci.*, *4*, 398–403, doi:10.1038/ngeo1129.

Ding, Q., E. J. Steig, D. S. Battisti, and J. M. Wallace (2012), Influence of the tropics on the Southern Annular Mode, *J. Clim.*, *25*, 6330–6363, doi:10.1175/JCLI-D-11-00523.1.

Fernandoy, F., H. Meyer, and M. Tonelli (2011), Stable water isotopes of precipitation and firn cores from the northern Antarctic Peninsula region as a proxy for climate reconstruction, *The Cryosphere Discuss.*, *5*, 951–1001, doi:10.5194/tcd-5-951-2011.

Fogt, R. L., and D. H. Bromwich (2006), Decadal variability of the ENSO teleconnection to the high-latitude South Pacific governed by coupling with the Southern Annual Mode, *Am. Meteorol. Soc.*, *19*, 979–997, doi:10.1175/JCLI3671.1.

Genthon, C., G. Krinner, and M. Sacchettini (2003), Interannual Antarctic tropospheric circulation and precipitation variability, *Clim. Dyn.*, *21*, 289–307, doi:10.1007/s00382-003-0329-1.

Genthon, C., S. Kaspari, and P. A. Mayewski (2005), Interannual variability of the surface mass balance of West Antarctica from ITASE cores and ERA40 reanalyses, 1958-2000, *Clim. Dyn.*, *24*, 759–770, doi:10.1007/s00382-005-0019-2.

Genthon, C., G. Krinner, and H. Castebrunet (2009), Antarctic precipitation and climate-change predictions: horizontal resolution and margin vs plateau issues, *Ann. Glaciol.*, *50*, 55–60.

Ginot, P., F. Stampfli, D. Stampfli, M. Schwikowski, and H. W. Gaggeler (2002), FELICS, a new ice core drilling system for high-altitude glaciers, *Mem. Nat`l. Inst. Polar Res.*, *56*, 38–48, doi:http://dx.doi.org/10.3189/172756409787769681.

Gow, A. J., and R. Rowland (1965), On the relationship of snow accumulation to surface topography at "Byrd Station", Antarctica, *J. Glaciol.*, *5*, 843–847.

Joughin, I., E. Rignot, C. E. Rosanova, B. K. Lucchitta, and J. Bohlander (2003), Timing of recent accelerations of Pine Island Glacier, Antarctica, *Geophys. Res. Lett.*, *30*(13), doi:10.1029/2003GL017609.

Joughin, I., B. E. Smith, and D. M. Holland (2010), Sensitivity of 21st century sea level to ocean-induced thinning of Pine Island Glacier, Antarctica, *Geophys. Res. Lett.*, *37*, L20502, doi:10.1029/2010GL044819.

Kaspari, S., P. D. Mayewski, D. A. Dixon, V. B. Spikes, S. Sneed B, M. J. Handley, and G. S. Hamilton (2004), Climate variability in West Antarctica derived from annual accumulation-rate records from ITASE firn/ice cores, *Ann. Glaciol.*, *39*, 585–594, doi:10.3189/172756404781814447.

Kavanaugh, J. L., and K. M. Cuffey (2003), Space and time-variation of δ18O and δD in Antarctic precipitation, revisited, *G. Bio. C.*, *17*, 1017 (2003).

Küttel, M., E. J. Steig, Q. Ding, A. J. Monaghan, and D. S. Battisti (2012), Seasonal climate information preserved in West Antarctic ice core water isotopes: relationships to temperature, large-scale circulation, and sea ice. *Clim. Dyn.*, *39*, 1841–1857, doi:10.1007/s00382-012-1460-7.

Lenaerts, J. T. M., M. R. van den Broeke, S. J. Déry, E. van Meijgaard, W. J. van de Berg, S. P. Palm, and J. Sanz Rodrigo (2012), Modeling drifting snow in Antarctica with a regional climate model: 1. Methods and model evaluation, *J. Geophys. Res.*, *117*, D05108, doi:10.1029/2011JD016145.

Manabe, S., and R. J. Stouffer (1980), Sensitivity of a global climate model to an increase of CO_2 concentration in the atmosphere, *J. Geophys. Res.*, *85*, 5529–5554, doi:10.1029/JC085iC10p05529.

Marshall, G. J. (2003), Trends in the Southern Annular Mode from observations and reanalyses, *J. Clim.*, *16*, 4134–4143, doi:10.1175/1520-0442.

Monaghan, A. J., et al. (2006a), Insignificant change in Antarctic snowfall since the International Geophysical Year, *Science*, *313*, 827–831, doi:0.1126/science.1128243.

Monaghan, A. J., D. H. Bromwich, and S. Wang (2006b), Recent trends in Antarctic snow accumulation from Polar MM5 simulations, *Phil. Trans. R. Soc.*, *364*, 1683–1708, doi:10.1098/rsta.2006.1795.

Morse, D. L., D. D. Blankenship, E. D. Waddington, and T. A. Neumann (2002), A site for deep ice coring in West Antarctica: results from aerogeophysical surveys and thermo-kinematic modeling, *Ann. Glaciol.*, *35*, 36–44, doi:10.3189/172756402781816636.

Noone, D., and I. Simmonds (2004), Sea ice control of water isotope transport to Antarctica and implications for ice core interpretation, *J. Geophys. Res.*, *109*, D07105, doi:10.1029/2003JD004228.

Oerlemans, J. (1982), Response of the Antarctic ice sheet to a climatic warming: a model study, *J. Climatol.*, *2*, 1–11, doi:10.1002/joc.3370020102.

Orsi, A. J., B. D. Cornuelle, and J. P. Severinghaus (2012), Little Ice Age cold interval in West Antarctica: Evidence from borehole temperature at the West Antarctic Ice Sheet (WAIS) Divide, *Geophys. Res. Lett.*, *39*, L09710, doi:10.1029/2012GL051260.

Parkinson, C. L., and D. J. Cavalieri (2012), Antarctic sea ice variability and trends, 1979-2010, *T.C.*, *6*, 871–880, doi:10.5914/tc-6-871-2012.

Rieneker, M. M., et al. (2011), MERRA: NASA's Modern-Era Retrospective Analysis for Research and Applications, *J. Clim.*, *24*, 3624–3648, doi:10.1175/JCLI-D-11-00015.1.

Rignot, E., J. L. Bamber, M. R. van den Broeke, C. Davis, Y. Li, W. J. van de Berg, and E. van Meijgaard (2008), Recent Antarctic ice mass loss from radar interferometry and regional climate modeling, *Nat. Geosci.*, *1*, 106–110, doi:10.1038/ngeo102.

Rignot, E., J. Mouginot, and B. Scheuchl (2011), Ice flow of the Antarctic ice sheet, *Science*, *333*, 1427–1430, doi:10.1126/science.1208336.

Schneider, D. P., Y. Okumura, and C. Deser (2012), Observed Antarctic Interannual climate variability and tropical linkages, *J. Clim.*, *25*(12), 4048–4066, doi:10.1175/JCLI-D-11-00273.1.

Siegert, M. J., and A. J. Payne (2004), Past rates of accumulation in central West Antarctica, *Geophys. Res. Lett.*, *31*, L12403, doi:10.1029/2004GL020290.

Steig, E., D. Schneider, S. Rutherford, M. Mann, J. Comiso, and D. Shindell (2009), Warming of the Antarctic ice-sheet surface since the 1957 International Geophyiscal Year, *Nature*, *457*, 459–462, doi:10.1038/nature07669.

Steig, E. J., Q. Ding, D. S. Battisti, and A. Jenkins (2012), Tropical forcing of Circumpolar Deep Water inflow and outlet glacier thinning in the Amundsen Sea Embayment, West Antarctica, *Ann. Glaciol.*, *53*, 19–28, doi:10.3189/2012AoG60A110.

Steig, E. J., et al. (2013), Recent climate and ice-sheet changes in West Antarctica compared with the past 2,000 years, *Nat. Geosci.*, doi:10.1038/ngeo1778.

Thomas, R., et al. (2004), Accelerated Sea-level rise from West Antarctica, *Science*, *306*, 255–258, doi:10.1126/science.1099650.

Thompson, D. W. J., S. Solomon, P. J. Kushner, M. H. England, K. M. Grise, and D. J. Karoly (2011), Signatures of the Antarctic ozone hole in Southern Hemisphere surface climate change, *Nat. Geosci.*, *4*, 741–749, doi:10.1038/NGEO1296.

Thompson, S., and D. Pollard (1997), Greenland and Antarctic mass balances for present and doubled atmospheric CO_2 from the Genesis Version-2 global climate model, *J. Clim.*, *10*, 871–899, doi:10.1175/1520-0442.

Turner, J., J. C. Comiso, G. J. Marshall, T. A. Lachlan-Cope, T. Bracegirdle, T. Maksym, M. P. Meredith, Z. Wang, and A. Orr (2009), Non-annular atmospheric circulation change induced by stratospheric ozone depletion and its role in the recent increase of Antarctic sea ice extent, *Geophys. Res. Lett.*, *36*, L08502, doi:10.129/2009GL037524.

Uppala, S. M., et al. (2005), The ERA-40 re-analysis, *Q. J. Roy. Meteorol. Soc.*, *131*(612), 2961–3012, doi:10.1256/qj.04.176.

Vaughan, D. G., J. L. Bamber, M. Giovinetto, J. Russel, and A. P. Cooper (1999), Reassessment of Net Surface Mass Balance in Antarctica, *J. Clim.*, *12*, 933–946, doi:10.1175/1520-0442(1999)012 < 0933:RONSMB > 2.0.CO.

Wallace, J. M., and P. V. Hobbs (1977), "Atmospheric Science: An Introductory Survey Academic Press", *New York*, 467.

Wingham, D. J., D. W. Wallis, and A. Shepherd (2009), Spatial and temporal evolution of Pine Island Glacier thinning, 1995-2006, *Geophys. Res. Lett.*, *36*, L17501, doi:10.1029/2009GL039126.

Winkelmann, R., A. Levermann, M. A. Martin, and K. Frieler (2012), Increased future ice discharge from Antarctica owing to higher snowfall, *Nature*, *492*, 239–242, doi:10.1038/nature11616.